SSRG International Journal of Electrical and Electronics Engineering
ISSN: 2348-8379/ https://doi.org/10.14445/23488379/IJEEE-V10I4P116

Volume 10 Issue 4, 164-168, April 2023

Original Article

Design and 3D Simulation of BAW Resonator for 5G

Poorvi. K. Joshi[1], Meghana. A. Hasamnis[2]

[1,2]*Shri Ramdeobaba College of Engineering and Management, Nagpur (MS), India.*

[1]*Corresponding Author : joshipk@rknec.edu*

Received: 04 March 2023 Revised: 31 March 2023 Accepted: 18 April 2023 Published: 30 April 2023

Abstract *- In this study, various materials like ZnO, PZT, BaTiO3, and LiNbO3 for piezoelectric thin-film are used to simulate Solidly Mounted Resonators (SMR). These materials have unique material characteristics that make them suitable for a specific application. High Q Factors are needed in communication systems for low noise and extremely sensitive signals. For the purpose of raising the SMR resonator's Q Factor, the various piezoelectric materials are examined. It is investigated how an SMR performs in connection to the stages of the Bragg reflector configuration and its constituent parts. Layers having low and high acoustic impedances, including SiO2/AlN, SiO2/W, SiO2/Mo, SiO2/ZnO and SiO2/Ta2O5, make up Bragg's reflector design. A comprehensive investigation of flexible SMR was conducted using COMSOL Multiphysics element method (FEM) simulations. The implications of the building phases and material used to make Bragg's reflectors on the functionality of the flexible SMR are thoroughly analyzed. Multiple Bragg's reflector designs' comparative results have been gathered and reported. W/SiO2-based Bragg's reflector topologies have been discovered in the most recent research with ZnO and are most suited to offer increased coupling coefficient and Quality Factor performance. It was found that 0.2 um, 0.3 um, and 0.1 um, respectively, were the best-optimized thicknesses for top metal electrodes, the piezoelectric layer, and the low and high acoustic impedance brag reflector layers. The current study's findings demonstrate that the simulated values of the coupling coefficient ($Keff^2$) and quality factor (Q) for the optimal dimension of the SMR structure are 0.09117 (or 9.117%) and 2335, respectively.*

Keywords *- Solidly Mounted Resonator(SMR), Quality Factor(Q), Coupling coefficient, Brag Reflector, Finite Element Machine (FEM).*

1. Introduction

Bulk acoustic resonators (BAW) are widely used in sensing applications because of their high sensitivity, quick measurement speed, straightforward design, and low design cost. [1]. Devices using bulk acoustic waves were developed later in 1980. [2]. BAW devices have frequently been produced on silicon substrates using the bulk micro-machining technique by inserting a piezo layer amongst thin metal layers. [3]. The piezoelectric effect creates the resonance of BAW resonators. When a BAW device is provided with an ac, acoustic waves are generated towards the electric field in a longitudinal direction [4]. The bottom electrode measures the longitudinal acoustic waves' backside reflection. Confinement within the piezoelectric layer causes due to perfect confinement of acoustic waves inside the BAW device. The reflection coefficient has a value of unity, allowing the acoustic wave to be completely confined. [5].

The acoustic velocity and the piezoelectric layer thickness are used to compute the fundamental resonance frequency of the BAW device. Provided by is the fundamental resonance frequency. [7]

$$f = \frac{\vartheta}{2tp} \qquad (1)$$

Here, tp and ϑ stand for the piezoelectric layer thickness and the acoustic wave velocity, respectively. In BAW devices, the thickness of the piezoelectric layer and fundamental resonance frequency are inversely correlated, according to equation (1). Parallel resonance occurs due to dielectric polarization and the acoustic wave when an out-of-phase situation occurs inside the resonator for a solidly mounted resonator (SMR) device [8].

BAW resonators classified as

1. Thin FBAR (figure 1)
2. SMR (figure 2)

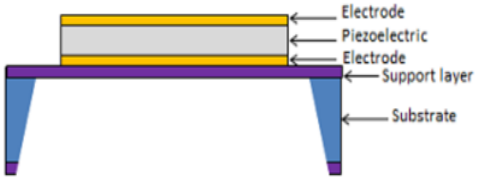

Fig. 1 Thin FBAR

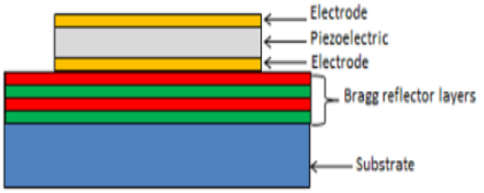

Fig. 2 SMR

Solidly mounted resonators are preferred because of their greater toughness, less mechanical damage during the dicing process, low layer tensions, and power handling capacities. Research on SMR so far is discussed below. Chengzhang Han at el, solidly mounted resonator (SMR) fabrication which can also function as a biological molecule sensor [9].Mohamed Mabrouk et al., for ladder BAW, a new customized interface tool for identifying parameters of Modified Butterworth-Van Dyke models [10]. R. Aigner et al., a summary of current BAW trends for high-frequency bands, broad bandwidth filters, miniaturization and thermal management. The development of complicated RF modules and their challenges are covered, as well as the evolution of RF content [12]. J. Olivares et al. explains how to create low-acoustic-impedance SiO2 films as a layer in Bragg mirrors for BAW resonators. Infrared absorption spectroscopy evaluates the material's composition and structure [13]. K.M. Lakin et al., Material interfaces are required for acoustic resonators, and these interfaces are commonly created at the electrodes using an air or vacuum interface. Another approach is to attach the resonator to a series of quarter-wavelength-thick layers to a substrate to create a solid for making low insertion loss GPS filters (SMR) [14].

M. A. Duboisa et al. created a solidly mounted resonator with a 10-layer acoustic reflector. They feature a strong resonance peak with a centre frequency of 2 GHz and a high Q factor with a k2 coupling coefficient of 1% [15]. K.M. Lakin et al. describe using high mechanical impedance electrodes to enhance the effective coupling coefficient of BAW resonators in SMR or FBAR designs. A better electrode arrangement that raises Ke2 (Effective coupling coefficient) for resonators has been developed, enabling the construction of broader bandwidth filters than would have been possible with electrodes made of solely aluminium [17]. Gayathri Pillai et al. suggested a composite thin-FBAR based on the apodization approach to permit the containment of displacement and strain energy at the resonator's centre section [18]. Wei-Che Shih et al. found that the changes made to the circuit according to the Mason model led to the device measurements. They studied the impact of different film conditions, material properties, and geometrical variations on the resonator's performance. [19] A. Volatier et al. introduced the FEMBEM technique to simulate two-dimensional SMR. They utilized the ATILA finite element program, which employs a discretized elastodynamic half-space Green function to describe the substrate.

[20] Roman Lanz et al.; developed bulk acoustic waves (BAW) resonators and filters that can operate at frequencies between 7 to 8 GHz, with quality factors ranging from 400 to 600 and coupling factors ranging from 4% to 5.5%. [21] S. Marksteiner et al.; devised a quantitative technique to optimize the layer stack of an acoustic mirror. With this approach, they were able to examine how the mirror structure influences the confinement of both longitudinal and shear wave energy. [23] A comprehensive analysis of resonators based on MEMS (Micro Electro Mechanical Systems). [24,25,26]
C. Cassella et al. has exhibited a novel type of monolithic RF passive components using cutting-edge cross-sectional Lamé-mode resonator (CLMR) technology based on aluminum nitride (AlN) MEMS.[27]R. Ruby et al. discuss the latest development in FBARs, the temperature-compensated zero-drift resonator (ZDR).[28]The crucial element in the design of MEMS filters is the resonators, which need to have specific characteristics such as high-quality factors, low internal loss and high-frequency stability to be effective.[29]

2. Proposed Work

2.1. The Paper's Novel Contribution

We are strongly motivated to employ various piezoelectric materials to overcome the aforementioned difficulties. In addition to the SiO2 layer, many materials are employed in brag reflectors. Some of the different piezoelectric materials utilized are BaTiO3, LiTaO3, PZT, and ZnO. In addition to the SiO2 layer, brag reflectors are made of AlN, ZnO, Mo, Ta2O5 and W. Comparisons are made between the performance study of SMR using various piezoelectric materials and the various materials utilized in brag reflectors in addition to SiO2 layer. The use of SMR with Tungsten (W) as one of the layers in the brag reflector and ZnO as the piezoelectric material has been found to yield a good Quality Factor. With its high resistance, this is because tungsten (W) allows for great energy confinement and isolation in SMR.

3. FEM Simulation and SMR Design

The top and bottom electrodes of the SMR are made of 200 nm thick aluminium, as shown in Figure 3. The Bragg reflector's high-low acoustic impedance layer is developed as a 100nm thick layer of various materials on top of a SiO2 layer.

3.1. Analysis of SMR's Quality Factors

Utilizing the COMSOL Multiphysics MEMS CAD tool, finite element simulation is conducted. Piezoelectric materials BaTiO3, LaTaO3, PZT, and ZnO are used to create a 3D model of the FBAR. First, 2D work planes with predetermined dimensions design the resonator.

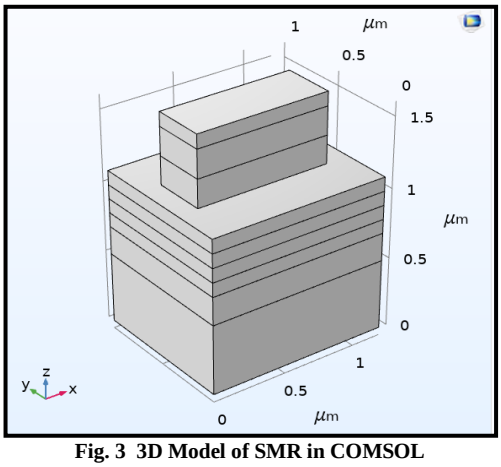

Fig. 3 3D Model of SMR in COMSOL

In contrast to the other plane used to create Brag reflector layers, the first two are utilized to create silicon substrate and oxide layers. The top and bottom electrodes that sandwich the piezoelectric material are used to design the whole resonator using the very next work plane.

The piezoelectric material is allocated to electrostatic physics, while solid mechanics physics is assigned to all other geometry domains. Figure 2 depicts the bottom and top electrodes as the resonator's ground and potential terminals. When 1mV of electric potential is given to the top electrode to activate the resonator, the geometry begins to resonate at a predetermined frequency determined via eigenfrequency analysis. The first eigenmode's frequency, 5.34 GHz, is where the resonator performs at its peak efficiency.

Below are the discussions on the different piezoelectric materials utilized for various feature sizes. Zno with dimensions of 800nm x 400nm, BaTiO3 with 1100nm x 350nm, LaTiO3 and PZT with 900nm x 350nm are considered while maintaining a Bragg reflector layer of SiO2/W, with a thickness of 100nm. The width of the Piezoelectric material is varied as 300nm, 140nm, 220nm, and 170nm for Zno, BaTiO3, LiTaO3, and PZT, respectively. The Quality Factor and Frequency for Zno are 2335 and 5.34GHz; for BaTiO3, they are 2010 and 5.345GHz; for LiTaO3, they are 1376 and 5.35GHz; and for PZT, they are 1007 and 5.335GHz, respectively. Zno demonstrates a higher quality factor in comparison to other piezoelectric materials, as has been noted. Figure 4 shows the simulated resonator's Quality factor (Q) for Zno.

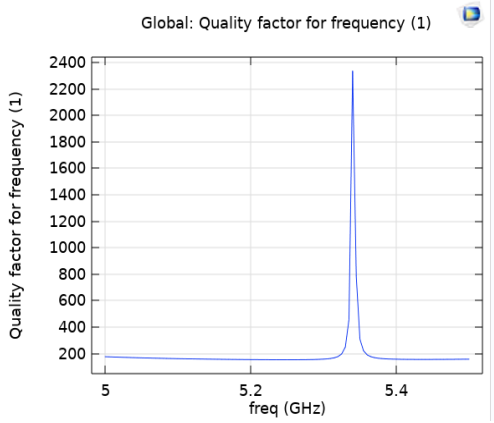

Fig. 4(a) Quality factor (Q) Vs Frequency

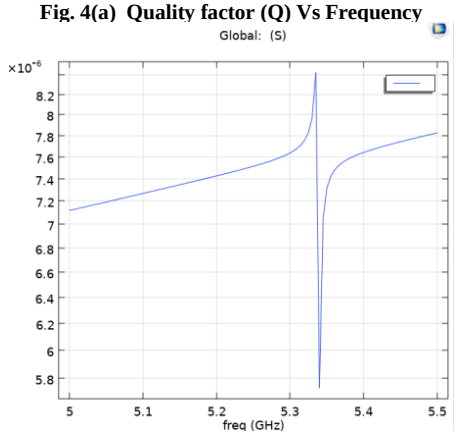

Fig. 4(b). Admittance Vs Frequency

3.2. Steps in the Micro-Fabrication Process

Micromechanical devices are constructed using lithographic patterning of films deposited on a substrate. Surface micromachining is a common type of manufacturing process. 2" silicon wafer that is p-type and has a <100> orientation (4–7 ohm-cm resistivity) is coated with a brag reflector (SiO2/W) isolation layer in two phases to begin the construction process. SiO2 has been deposited using both wet oxidation and CVD. Thermal evaporation (200 nm) is employed for metal deposition (Al) to create the bottom electrode. Following that, a first-level electron beam lithography with a bottom electrode is carried out. Following etching with an aluminium etchant, piezoelectric ZnO-sputter depositing (300nm). Etching of ZnO in second-level electron beam lithography (MASK 2). SiO2 (a 600 nm spacer layer) is being deposited. Third-year Lithography (Mask 3). SiO2 etching. Al-based metal deposition for thermal evaporation-based top electrode creation (200nm). Al-based metal deposition for thermal evaporation-based top electrode creation (200nm). The microfabrication process steps are shown in Figure 5.

Fig. 5(a) RCA, Wet oxidation, deposition of tungsten

Fig. 5(b) Deposition of SiO_2, tungsten

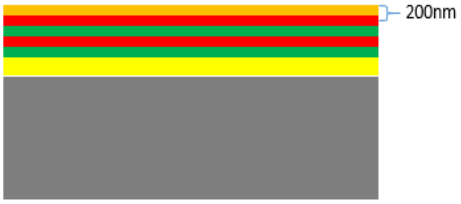

Fig. 5(c) Sputtering of aluminium

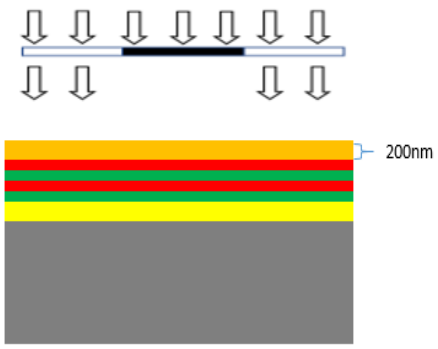

Fig. 5(d) 1st level lthography (Mask 1)

Fig. 5(e) Etching of aluminium

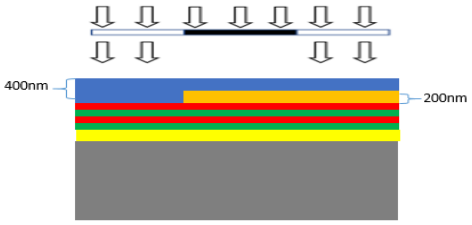

Fig. 5(f) Deposition of piezoelectric layer, 2nd level lithography (Mask 2)

Fig. 5(g) Etching of piezolayer, deposition of SiO_2 (Spacer Layer)

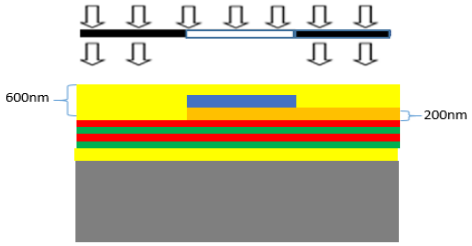

Fig. 5(h) 3rd level lithography (Mask3)

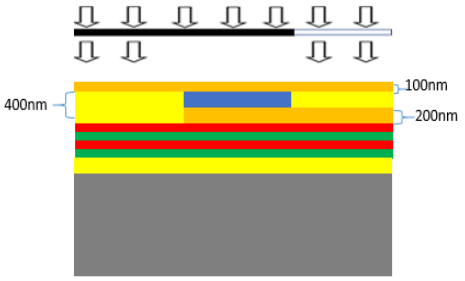

Fig. 5(i) Sputtering of aluminium

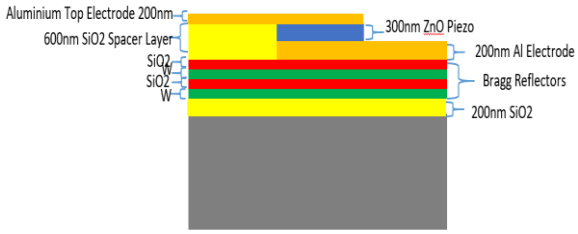

Fig. 5(j) Device 4th level lithography (Mask 4)
Fig. 5 Process flow for fabrication

4. Results and Discussions

In the presented study, various piezoelectric thin-film materials, such as ZnO, PZT, BaTiO3, and LiNbO3, are used to simulate Solidly Mounted Resonators (SMR). Every one of these materials has unique material characteristics that make it suitable for a specific purpose. High Q Factors are needed in communication systems for low noise and extremely sensitive signals. For the purpose of raising the SMR resonator's Quality Factor, the various piezoelectric materials are examined. It is investigated how an SMR performs in connection to the stages of the Bragg reflector configuration and its constituent parts. Layers having low and high acoustic impedances, including SiO2/W, SiO2/AlN, SiO2/Mo, SiO2/Ta2O5, and SiO2/ZnO, make up Bragg's reflector design. Using COMSOL 5.6 Multiphysics simulation, the FBAR Resonator was modelled.

5. Conclusion

According to a recent study, Bragg's reflector designs built on ZnO and W/SiO2 are most suited to provide improved performance in terms of Quality Factors. The optimization process was undertaken with the goal of raising SMR's Quality Factor. The brag reflector's top metal electrodes, a piezoelectric layer, and low- and high-acoustic impedance layers were all found to be best optimized at 0.2 micrometers, 0.3 micrometers, and 0.1 micrometers, respectively. The results of the current investigation show that the quality factor (Q) and coupling coefficient ($Keff^2$) simulation values for the optimal dimension of the SMR structure are 0.09117 (or 9.117%) and 2335, respectively.

References

[1] D. L. Polla, "MEMS Technology for Biomedical Applications," *6th International Conference on Solid-State and Integrated Circuit Technology. Proceedings (Cat. no.01EX443)*, vol. 1, pp. 19-22, 2001. [CrossRef] [Google Scholar] [Publisher Link]

[2] K.M. Lakin, and J.S. Wang, "UHF Composite Bulk Wave Resonators," *Ultrasonics Symposium*, pp. 834-837, 1980. [CrossRef] [Google Scholar] [Publisher Link]

[3] H.P. Löbl et al., "Materials for Bulk Acoustic Wave (BAW) Resonators and Filters," *Journal of the European Ceramic Society*, vol. 21, no. 15, pp. 2633-2640, 2021. [CrossRef] [Google Scholar] [Publisher Link]

[4] Lu, Y., Emanetoglu, N.W. and Chen, Y., "Zno Piezoelectric Devices. in Zinc Oxide Bulk, Thin Films and Nanostructures: Processing. Properties, and Applications," pp. 443-489, 2007. [CrossRef] [Google Scholar] [Publisher Link]

[5] Sumy Jose et al., "*Reflector Stack Optimization for Bulk Acoustic Wave Resonators*," 2011, [CrossRef] [Google Scholar] [Publisher Link]

[6] Dr. K. G. Neerajakshi, "Thermodynamic and Acoustic Properties of Binary Mixtures of PEGDME 200 with 1-Propanol," *SSRG International Journal of Applied Chemistry*, vol. 7, no. 3, pp. 33-37, 2020. [CrossRef] [Publisher Link]

[7] P. K. Joshi, K. R. Latwe, and M. A. Hasamnis, "Analysis and Enhancement of Q-Factor in Thin-Film Bulk Acoustic Wave Resonator (FBAR)," *2022 Journal of Physics: Conference Series*, vol. 2273, 2022. [CrossRef] [Google Scholar] [Publisher Link]

[8] F.H. Villa Lopez et al., “Design and Modelling of Solidly Mounted Resonators for Low-Cost Particle Sensing,” *Measurement Science and Technology*, vol. 27, no. 2, p. 025101, 2015. [CrossRef] [Google Scholar] [Publisher Link]

[9] Chengzhang Han et al., “Solidly Mounted Resonator Sensor for Biomolecule Detections,” *RSC Advances*, vol. 9, no. 37, pp. 21323-21328, 2019. [Google Scholar] [Publisher Link]

[10] Mabrouk Mohamed et al., "Flexible Engineering Tool for Radiofrequency Parameter Identification of RF-MEMS BAW Filters,” *ETRI Journal*, vol. 38, no. 5, 2016, pp. 988-995, 2016. [CrossRef] [Google Scholar] [Publisher Link]

[11] R. Hari Setyanto et al., "Investigation of the Helmholtz Green Resonator Panel from Rice Husk Waste and Office Paper Reinforced With Coconut Coir Skin as a Noise Absorbing Panel," *International Journal of Recent Engineering Science,* vol. 6, no.1, pp. 1-4, 2019. [CrossRef] [Google Scholar] [Publisher Link]

[12] R. Aigner et al., "BAW Filters for 5G Bands," *IEEE International Electron Devices Meeting (IEDM),* pp. 14.5.1-14.5.4, 2018. [CrossRef] [Google Scholar] [Publisher Link]

[13] J. Olivares et al., "Sputtered Sio2 as Low Acoustic Impedance Material for Bragg Mirror Fabrication in BAW Resonators," *2009 IEEE International Frequency Control Symposium Joint With the 22nd European Frequency and Time Forum*, pp. 316-321, 2009. [CrossRef] [Google Scholar] [Publisher Link]

[14] K. M. Lakin, K. T. Mccarron, and R. E. Rose, "Solidly Mounted Resonators and Filters," *1995 IEEE Ultrasonics Symposium. Proceedings. An International Symposium,* vol. 2, pp. 905-908, 1995. [CrossRef] [Google Scholar] [Publisher Link]

[15] M.-A. Dubois et al., "Solidly Mounted Resonator Based on Aluminum Nitride Thin Film," *1998 IEEE Ultrasonics Symposium. Proceedings* (Cat. no. 98CH36102), pp. 909-912, 1998. [CrossRef] [Google Scholar] [Publisher Link]

[16] Rohit Kumar Saini, "Design and Study of the Effect of Stub At the Tip of Simple, Stacked Triangular Patch With and Without Air Gap," *SSRG International Journal of Electronics and Communication Engineering*, vol. 8, no. 5, pp. 11-15, 2021. [CrossRef] [Publisher Link]

[17] K. M. Lakin et al., "Improved Bulk Wave Resonator Coupling Coefficient for Wide Bandwidth Filters," *2001 IEEE Ultrasonics Symposium. Proceedings. An International Symposium (Cat. no.01CH37263),* pp. 827-831, 2001. [CrossRef] [Google Scholar] [Publisher Link]

[18] Gayathri Pillai et al., "Design and Optimization of SHF Composite FBAR Resonators," *IEEE Transactions on Ultrasonics, Ferroelectrics, and Frequency Control*, vol. 64, no. 12, pp. 1864-1873, 2017. [CrossRef] [Google Scholar] [Publisher Link]

[19] Wei-Che Shih et al., "Simulation of Solidly Mounted Resonator Using Mason Model and Its Implementation,” *Sensors and Materials*, 2017, vol. 29, no. 4, pp. 405-410, 2016. [CrossRef] [Google Scholar] [Publisher Link]

[20] Volatier, B. Dubus, and D. Ekeom, "P1J-7 Solidly Mounted Resonator (SMR) FEM-BEM Simulation," *2006 IEEE Ultrasonics Symposium*, pp. 1474-1477, 2006. [CrossRef] [Google Scholar] [Publisher Link]

[21] R. Lanz, M. -A. Dubois, and P. Muralt, "Solidly Mounted BAW Filters for the 6 To 8 GHz Range Based on ALN Thin Films," *2001 IEEE Ultrasonics Symposium. Proceedings. An International Symposium (Cat. no.01CH37263),* vol. 1 pp. 843-846, 2001. [CrossRef] [Google Scholar] [Publisher Link]

[22] Rahul Khadase et al., "In Vitro Testing of Implantable Antenna for Glucose Sensing," *International Journal of Engineering Trends and Technology*, vol. 69, no. 7, pp. 109-113, 2021. [CrossRef] [Publisher Link]

[23] S. Marksteiner et al., "Optimization of Acoustic Mirrors for Solidly Mounted BAW Resonators," *IEEE Ultrasonics Symposium*, pp. 329-332, 2005. [CrossRef] [Google Scholar] [Publisher Link]

[24] Reza Abdolvand et al., "Micromachined Resonators: A Review," *Micromachines*, vol. 7, no. 9, p. 160, 2016. [CrossRef] [Google Scholar] [Publisher Link]

[25] Linlin Wang et al., “A Review on Coupled Bulk Acoustic Wave MEMS Resonators,” *Sensors*, vol. 22, no. 10, p. 3857, 2022. [CrossRef] [Google Scholar] [Publisher Link]

[26] Gayathri Pillai, and Sheng-Shian Li, "Piezoelectric MEMS Resonators: A Review," *IEEE Sensors Journal*, vol. 21, no. 11, pp. 12589-12605, 2021. [CrossRef] [Google Scholar] [Publisher Link]

[27] Cristian Cassella et al., "RF Passive Components Based on Aluminum Nitride Cross-Sectional Lamé-Mode MEMS Resonators," *IEEE Transactions on Electron Devices*, vol. 64, no. 1, pp. 237-243, 2017. [CrossRef] [Google Scholar] [Publisher Link]

[28] Rich Ruby et al., "Positioning FBAR Technology in the Frequency and Timing Domain," *IEEE Transactions on Ultrasonics, Ferroelectrics, and Frequency Control*, vol. 59, no. 3, pp. 334-345, 2012. [CrossRef] [Google Scholar] [Publisher Link]

[29] Setoudeh, Farbod, “A Novel Structure for Design and Simulation of a MEMS Resonator for Biomedical Applications,” *Biomedical Journal of Scientific & Technical Research*, vol. 20, no. 2, pp. 14910-14914, 2019. [CrossRef] [Google Scholar] [Publisher Link]